

# 实验室模拟研究硫酸铵和甘氨酸对乙醇醛与胺反应体系生成棕碳的影响

孙娟<sup>1#</sup>, 丁喆正<sup>1#</sup>, 易雅谊<sup>2</sup>, 陈彦奇<sup>1</sup>, 薛丽坤<sup>1</sup>, 王文兴<sup>1</sup>, 周学华<sup>1\*</sup>

1. 山东大学 环境研究院, 青岛 266237

2. 青岛众瑞智能仪器股份有限公司, 青岛 266237

**摘要:** 二次有机气溶胶是有机气溶胶的重要组成部分。大气中羰基化合物与胺/铵反应可以产生吸光性有机气溶胶(如棕碳), 对大气辐射和全球气候产生深刻影响。本文模拟研究了大气中硫酸铵和甘氨酸对乙醇醛与胺(如甲胺、甘氨酸)反应生成棕碳的影响。通过对反应溶液紫外-可见吸收光谱和反应动力学分析, 发现硫酸铵对反应体系棕碳的生成起抑制作用, 而甘氨酸和甲胺的混合可以协同促进棕碳生成; 通过对产物进行质谱分析, 发现反应机理主要为半缩醛/缩醛反应以及含氮化合物的亲核加成; 通过对产物有机碳进行分析, 发现当硫酸铵参与反应时, 有利于大分子二次有机碳生成。这些发现对棕碳在大气中的形成途径、乙醇醛在化学模型中对棕碳形成的贡献以及对大气中其他羰基行为的预测具有重要意义。

**关键词:** 二次有机气溶胶; 棕碳; 实验室模拟; 乙醇醛; 硫酸铵; 甘氨酸; 甲胺

## The opposing influences of ammonium sulfate/glycine on the formation of brown carbon in glycolaldehyde with amine system in a laboratory simulation

SUN Juan<sup>1#</sup>, DING Zhezhen<sup>1#</sup>, YI Yayi<sup>2</sup>, CHEN Yanqi<sup>1</sup>, XUE Likun<sup>1</sup>, WANG Wenxing<sup>1</sup>, ZHOU Xuehua<sup>1\*</sup>

1. Environment Research Institute, Shandong University, Qingdao 266237, China

2. Qingdao Junray Intelligent Instrument Co., Ltd., Qingdao 266108, China

**Abstract: Background, aim, and scope** Secondary organic aerosols (SOA) are important parts of organic aerosols. The reaction of carbonyl compounds with amine/ammonium can generate light-absorbing organic aerosol (i.e., brown carbon (BrC)) in the atmosphere, which affects both radiative forcing and global climate. This reaction has become an important aspect of atmospheric chemistry. In the aqueous reaction of glycolaldehyde (Gald) with amine/ammonium to form BrC, we aim to explore the different effects of ammonium sulfate (AS)/

收稿日期: 2021-12-11; 录用日期: 2022-03-07; 网络出版: 2022-03-19

Received Date: 2021-12-11; Accepted Date: 2022-03-07; Online first: 2022-03-19

基金项目: 国家自然科学基金项目(21507070, 91544213)

Foundation Item: National Natural Science Foundation of China (21507070, 91544213)

通信作者: 周学华, E-mail: xuehuazhou@sdu.edu.cn

Corresponding Author: ZHOU Xuehua, E-mail: xuehuazhou@sdu.edu.cn

引用格式: 孙娟, 丁喆正, 易雅谊, 等. 2022. 实验室模拟研究硫酸铵和甘氨酸对乙醇醛与胺反应体系生成棕碳的影响 [J]. 地球环境学报, 13(2): 226-239.

Citation: Sun J, Ding Z Z, Yi Y Y, et al. 2022. The opposing influences of ammonium sulfate/glycine on the formation of brown carbon in glycolaldehyde with amine system in a laboratory simulation [J]. *Journal of Earth Environment*, 13(2): 226-239.

# 这些作者贡献和排名相同。

These authors contributed equally to this work and should be considered co-first authors.

glycine (Gly) on the formation of BrC in this reaction system. **Materials and methods** Glycolaldehyde is the simplest hydroxycarbonyl compound in the atmosphere. We examined the ultraviolet-visible absorbance spectra, reaction kinetics, and the secondary organic carbon (SOC) masses of the mixed solutions of GALd. Moreover, we employed time-of-flight and ion trap mass spectrometry (LCMS-IT-TOF) to determine the reaction products. **Results** The results demonstrated that the absorbance and reaction rate of the products followed the order of GALd+methylamine (MA)+AS < GALd+MA, GALd+Gly+AS < GALd+Gly, GALd+MA+Gly > GALd+MA or GALd+Gly. Compared with the reaction of GALd with either MA or Gly, the GALd+MA+AS, GALd+Gly+AS, and GALd+MA+Gly reactions are increasingly favorable to produce the aqueous SOC. Furthermore, it was apt to form high-molecular-weight SOC with when AS participated in the reaction. **Discussion** After adding AS and Gly to the reaction system of GALd with amine, the two substances have opposite effects on BrC formation in the reaction system. These effects might be attributed to the changes of pH in the solutions, additional concentration variations of reactants with nitrogen (e.g.,  $\text{NH}_3$ ,  $\text{CH}_3\text{NH}_2$ , and  $\text{H}_2\text{NCH}_2\text{COO}^-$ ), and the participation of  $\text{NH}_3$  and  $\text{H}_2\text{NCH}_2\text{COO}^-$  in the reactions of GALd with amine after the addition of AS in GALd+MA or GALd+Gly and Gly in GALd+MA. In the GALd+MA+AS, GALd+Gly+AS reaction systems, AS reduces the pH value of the solution, thereby reducing the concentration of reactants and inhibiting the formation of BrC; in the GALd+MA+Gly reaction system, organic amines and inorganic ammonium jointly promote the formation of BrC. In the reaction process, the main reaction mechanism is the hemiacetal/acetal reaction of GALd, followed by nucleophilic addition reaction with nitrogen-containing substances to generate high molecular weight oligomers. Moreover, the mixed reaction systems can produce more secondary organic carbon than GALd with single MA and Gly. **Conclusions** The reaction rate agrees with the UV absorption, showing that AS inhibits BrC formation and the mixing of Gly and MA promotes BrC formation. The primary reaction mechanism is the hemiacetal/acetal reaction and nucleophilic attack. When AS participates in these reactions, it is conducive to the formation of macromolecular products. **Recommendations and perspective** The results have considerable implications on BrC formation in the atmosphere, the contribution of GALd to BrC formation in chemical models, and the predictions of the behaviors of other carbonyls in the atmosphere.

**Key words:** secondary organic aerosol; brown carbon; laboratory simulation; glycolaldehyde; ammonium sulfate; glycine; methylamine

Brown carbon (BrC) is becoming a concern in atmospheric research because organic carbon (OC) only scatters solar radiation with negative forcing. Atmospheric BrC is known to have multiple sources, including primary emissions from biomass burning (Kirchstetter et al, 2004; Hecobian et al, 2010; Lack et al, 2012; Kawamura et al, 2013), fossil fuel combustion (Bond, 2001; Zhang et al, 2011), and vehicle exhaust and secondary formation via various mechanisms such as the ozonolysis of terpenes, subsequent aging in the presence of ammonium ions (Bones et al, 2010) or reactions of carbonyls/aromatic compounds with nitrogenous substances (Laskin et al, 2015). Among these reactions, water-soluble carbonyl compounds with ammonium salts, amino acids, such as

glycine (Gly), or primary amines, such as methylamine (MA), can undergo Maillard-type browning or aldol condensation reactions to form secondary organic aerosols (SOA) (Hastings et al, 2005; de Haan et al, 2009; de Haan, 2011). Moreover, other researchers observed that the Maillard reaction in the atmosphere confirms the presence of the actual atmospheric environment (Chen et al, 2021a; Chen et al, 2021b; Tang et al, 2021). Based on constraints on the global deposition of OC, Goldstein and Galbally (2007) estimated that  $>175 \text{ Tg} \cdot \text{a}^{-1}$  (in carbon) is deposited on the Earth's surface as SOA. The global emission of SOA from the irreversible uptake of dicarbonyls is  $11 \text{ Tg} \cdot \text{a}^{-1}$  (in carbon), 90% of which occurs in clouds (Fu et al, 2008). Note that these

SOA products have considerable influence on aerosol optical properties because of the production of BrC (Powelson et al, 2014). Shapiro et al (2009) proposed that the aldol condensation and oligomerization of glyoxal were responsible for forming light-absorbing products in the reactions of glyoxal/ammonium sulfate (AS) solution, and Bones et al (2010) examined the formation of strong absorbers and fluorophores in the products of limonene-O<sub>3</sub> SOA. Currently, multiple carbonyl compounds (such as glyoxal, methylglyoxal, acetaldehyde, and hydroxyacetone) have been reported in reactions with either ammonium or amine (Galloway et al, 2009; Shapiro et al, 2009; Schwier et al, 2010; Yu et al, 2011; Yi et al, 2018a; de Haan et al, 2020; Jimenez et al, 2022). Nitrogen in amine (MA, Gly), as a nucleophile, is more active in attacking the carbenium in carbonyl compounds (Galano et al, 2004; de Haan et al, 2018; Yi et al, 2018a). What happens when AS or Gly is added in the reaction of carbonyl compounds and amine? This question inevitably arises in the real atmospheric environment and is rarely investigated.

In atmospheric chemistry, glycolaldehyde (GAlD), the simplest hydroxycarbonyl, is an important compound, which can be directly emitted by biomass burning or formed by the oxidation of volatile organic compounds (Bacher et al, 2001; Kua et al, 2013). In the atmosphere, GAlD was reported at mid-part-per-trillion to low-part-per-billion mixing ratios in the gas and atmospheric aqueous phases such as clouds, fog, and aqueous aerosol (Zhou et al, 2009). In the gas phase, hydroxyl (OH) radical oxidation and photolysis are the dominant loss processes of GAlD, causing an atmospheric lifetime of only several hours to a day (Bacher et al, 2001; Spaulding et al, 2003). The photolysis of GAlD in the condensed phase is considerably less relevant than the aqueous phase because about 90% of GAlD is reported in the hydrated, existing gem-diol form rather than the more reactive aldehyde form (Sørensen, 1972; Bacher et al, 2001). The aqueous phase oxidation of GAlD by OH radicals can form glyoxal and oxidized acids (e.g., oxalic, glyoxylic, and glycolic) (Warneck, 2003; Perri

et al, 2009). GAlD has the potential to form BrC with ammonium salts/amines via nonoxidative liquid-phase reactions (Powelson et al, 2014). In BrC formation, the reaction of GAlD with amines had far faster rates than that of GAlD with AS (Yi et al, 2018a). However, the influences of AS or Gly on the reactions of GAlD with amine are not understood well.

In this study, under dark conditions, the variations of light-absorbing secondary OC (SOC) products from the reactions of GAlD with MA/Gly in the aqueous phase after AS was added and from the reaction of GAlD with MA after Gly was added were investigated at  $(275 \pm 2)$  K. The ultraviolet-visible (UV-vis) absorbance spectra of products were monitored for reaction kinetics and optical characteristics. The solution pH was inspected before and after AS or Gly was added in the reaction of GAlD with amines. Moreover, time-of-flight and ion trap mass spectrometry (LCMS-IT-TOF) was employed to determine the reaction products and confirm the reaction mechanisms. Finally, the produced SOC masses were evaluated.

## 1 Materials and methods

### 1.1 Sample preparation

All chemicals were purchased from Aladdin unless otherwise designated, including GAlD dimer (Sigma-Aldrich), AS (AR,  $\geq 99.0\%$ ), Gly (AR, 98%), and MA (Aladdin, 40% in water). The reactions of  $0.2 \text{ mol} \cdot \text{L}^{-1}$  GAlD +  $0.25 \text{ mol} \cdot \text{L}^{-1}$  MA +  $0.25 \text{ mol} \cdot \text{L}^{-1}$  AS,  $0.2 \text{ mol} \cdot \text{L}^{-1}$  GAlD +  $0.25 \text{ mol} \cdot \text{L}^{-1}$  Gly +  $0.25 \text{ mol} \cdot \text{L}^{-1}$  AS, and  $0.2 \text{ mol} \cdot \text{L}^{-1}$  GAlD +  $0.25 \text{ mol} \cdot \text{L}^{-1}$  MA +  $0.25 \text{ mol} \cdot \text{L}^{-1}$  Gly were performed at a constant temperature and in a humidity chamber at  $(275 \pm 2)$  K (Powelson et al, 2014). Moreover, the contrasting experiments, the reactions of  $0.2 \text{ mol} \cdot \text{L}^{-1}$  GAlD +  $0.25 \text{ mol} \cdot \text{L}^{-1}$  AS,  $0.2 \text{ mol} \cdot \text{L}^{-1}$  GAlD +  $0.25 \text{ mol} \cdot \text{L}^{-1}$  MA, and  $0.2 \text{ mol} \cdot \text{L}^{-1}$  GAlD +  $0.25 \text{ mol} \cdot \text{L}^{-1}$  Gly were performed under the same condition.

### 1.2 Analytical methods

The experiments were performed in glass vials wrapped with Al foil to avoid exposure to light and then placed in a constant temperature and humidity

chamber (BPHS-060A, Shanghai Yiheng Technology Instrument Co., Ltd.,) with the temperature at  $(275 \pm 2)$  K. A UV-vis spectrophotometer (TU-1900, Beijing Purkinje General Instrument Co., Ltd.,) recorded changes in absorbance between 190 nm and 900 nm with 1-mm-sized cuvettes of quartz.

Absorbance data were converted to mass absorption coefficients (MAC, in  $\text{cm}^2 \cdot \text{g}^{-1}$ ) using the following equation (Nozière and Esteve, 2007):

$$\text{MAC} = \text{Abs}_e(\lambda) / b \times C_{\text{mass}} \quad (1)$$

where  $\text{Abs}_e$  is base e absorbance at wavelength  $\lambda$ ,  $b$  is the path length in cm, and  $C_{\text{mass}}$  is the total concentration of reactants in  $\text{g} \cdot \text{cm}^{-3}$ .

Online electrospray ionization tandem mass spectroscopy (ESI-MS) was performed on an ion trap-time of flight hybrid mass spectrometer (Shimadzu, Japan). ESI-MS analysis was set in the negative or positive ion mode (Yi et al, 2018a; Yi et al, 2018b). The mass acquisition range was 50—500.

A thermal-optical transmittance carbon analyzer (Sunset Laboratory Tigrard, OR, USA) was used to determine the OC under a modified version of the NIOSH protocol (Birch and Cary, 1996). The reaction solution (10  $\mu\text{L}$ ) was introduced into preheated quartz filters ( $1 \times 1.5 \text{ cm}^2$ , Pallflex, Tissuquartz 2500 QAT-UP) using a syringe. In the first stage, the oven temperature was increased to 1143 K in pure He to thermally volatilize OC; then, the temperature was reduced to 823 K, and oxygen/helium (10 : 90) was introduced, and finally the oven was heated to 1143 K for thermal oxidization of element carbon (EC).

A pH meter (Five Easy Plus, FE28-Standard, Mettler-Toledo Instruments, Shanghai) was employed to monitor the solution pH.

### 1.3 Reaction kinetics

Kinetic data were obtained based on the Beer-Lambert law. The sample absorbance ( $A_b(\lambda)$ ) was converted in extinction coefficient ( $\varepsilon_i$ ) (Eq. (2)), and the absorption indices ( $A_i$ ) were calculated using Eq. (3) for direct comparison with the optical properties of atmospheric aerosols.

$$\varepsilon_i = \frac{A_b(\lambda)}{l} \quad (2)$$

$$A_i = \frac{\lambda \varepsilon_i}{4\pi} \quad (3)$$

Reactions obeying the first-order kinetics were fitted using Eq. (4), and the corresponding rate constants ( $k^1$  ( $\text{s}^{-1}$ )) were obtained from the slope of Eq. (5).

$$\varepsilon_i(t) = \varepsilon_\infty (1 - e^{-k^1 t}) \quad (4)$$

$$\ln(1 - \frac{\varepsilon_i}{\varepsilon_\infty}) = -k^1 t \quad (5)$$

where  $\lambda$  is the wavelength,  $l$  is the optical path length ( $l = 0.1 \text{ cm}$ ), and  $\varepsilon_\infty$  is the reaction mixture absorption after a long time (i.e., at a high degree of conversion) (Nozière and Esteve, 2007).

## 2 Results and Discussion

### 2.1 UV-vis absorption of products

Fig. 1 shows the UV-vis absorption spectra of background solution GAlD(a), AS(b), Gly(c), and MA(d). Fig. 2a shows the absorption of products from GAlD+MA+AS, GAlD+MA, and GAlD+AS reactions. From the figure, in the GAlD+MA reaction, in addition to the absorption at about 216 nm, there was another peak at about 330 nm, attributable to imine and carbonyl group-containing in the production (Yu et al, 2011). However, there was an obvious decrease for absorption at  $>300 \text{ nm}$  after AS was added, indicating that AS had an inhibitory effect on the BrC formation in the GAlD+MA reaction. In Fig. 2b, the GAlD+Gly reaction demonstrated similar absorption peaks at about 216 nm and 330 nm to that from GAlD+MA. After AS was added in the GAlD+Gly reaction, the absorption peak at 330 nm was slightly lower than that of the GAlD+Gly reaction, indicating that AS had an inconspicuous inhibitory effect on the BrC production in the GAlD+Gly reaction. Unlike AS, after Gly was added in the GAlD+MA reaction, the absorption peak at about 330 nm was far higher than that of the GAlD reaction with either MA or Gly (Fig. 2c). Moreover, the GAlD+MA+Gly reaction exceeded the UV-vis spectral range after 9 h, which indicates that the addition of Gly into the GAlD+MA reaction caused an accelerated formation of BrC, thus indicating a synergistic effect of Gly and MA.

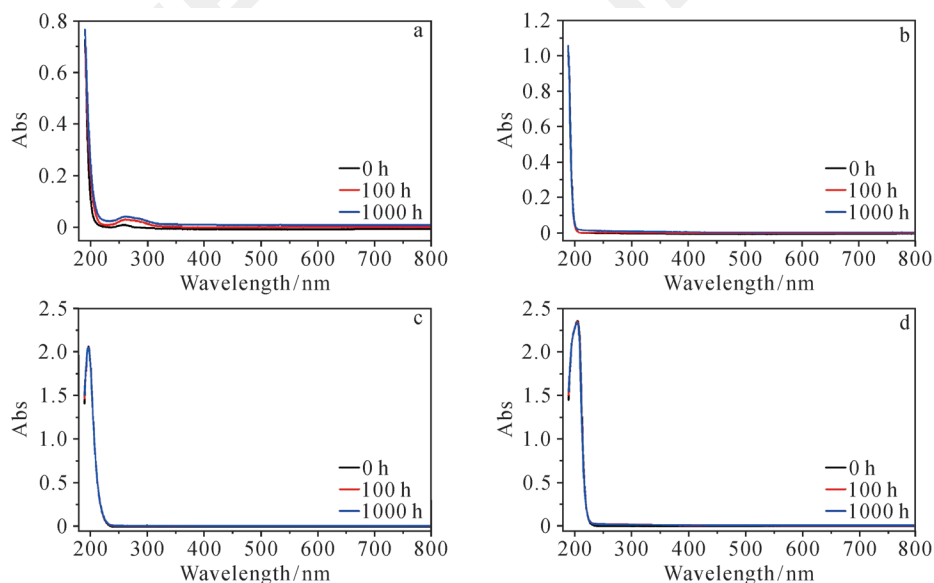


Fig. 1 UV-vis absorption spectra of background solutions GALd (a), AS (b), Gly (c) and MA (d)

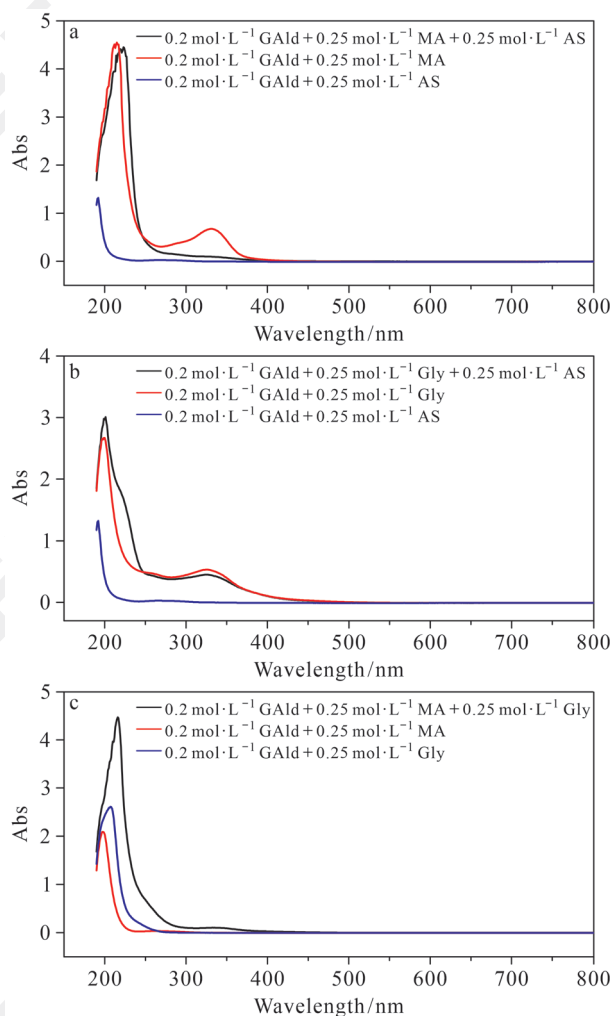


Fig. 2 The comparison of UV-vis absorption after AS was added into the GALd+MA reaction of in 7 d (a), after AS was added into the GALd+Gly reaction in 7 d (b), and after Gly was added into the GALd+MA reaction in 4 h (c)

## 2.2 Reaction kinetics

The reaction kinetics was analyzed based on the absorbance of reaction products measured by the UV-vis spectra. The GALd + MA + AS, GALd + MA, GALd + Gly + AS, GALd + Gly, and GALd + MA + Gly reactions were first-order reactions, which agreed with a previous study (Yi et al, 2018a). The rate constants at about 216 nm and 330 nm are listed in Tab. 1. After AS was added into the GALd+MA reaction, the rate constant of GALd+MA+AS had the same order of magnitude as that of GALd+MA but lower values with factors of 0.71 and 0.61 at 216 nm and 330 nm, respectively, although the reactant (MA + AS) concentrations increased because of the AS added compared with GALd+MA. This suggested that AS could decrease the reaction rate of GALd+MA. The pH of AS is  $(5.45 \pm 0.06)$  based on Reaction (1), and the solution of MA has a high pH of  $(12.0 \pm 0.20)$  because of Reaction (2). Fig. 3 shows the pH of the GALd+MA+AS and GALd+MA solutions. From the figure, after AS was added to the GALd+MA reaction, according to Reaction (1),  $\text{NH}_4^+$  was ionized in  $\text{NH}_3$  and  $\text{H}^+$ , decreasing the pH of the solution. The decreased pH might reduce the reaction of GALd with MA (Yi et al, 2018b). The rate constants of GALd+Gly+AS at 216 nm and 330 nm were 0.76 and 0.77 times those of GALd+Gly, respectively. The AS and GALd+Gly solutions had near pH values. After

AS was added into the GALd+Gly solution, the pH was almost unchanged (Fig. 3); Reactions (1) and (3) can ionize  $H^+$ ; therefore, the influence of AS on the GALd+Gly reaction was minute. In comparison, the rate constant of the GALd+MA+Gly reaction was higher than that of GALd+MA or GALd+Gly at both 216 nm and 330 nm, even 32 and 19 times the sums at the two wavelengths, respectively. This showed that the mixtures of Gly and MA solutions significantly accelerated the reaction and favored the BrC formation. From Fig. 3, after Gly was added in the GALd+MA solution, the pH of the solution decreased because of Reaction (3). The decreased pH might decrease the reaction of a carbonyl compound with MA (Yi et al, 2018b). However, for the GALd+Gly solution, the pH increased when it was mixed with MA (Reaction (3)), particularly with a considerably jump from weak acidity to strong alkalinity, which might yield an explosive BrC formation. In the alkaline solution, the GALd+Gly reaction could produce BrC with high absorbance (Fig. 4).

The pH of the  $0.25 \text{ mol} \cdot \text{L}^{-1}$  GALd+ $0.25 \text{ mol} \cdot \text{L}^{-1}$  Gly reaction was adjusted to 9.43 with NaOH, close to the value of  $(9.47 \pm 0.10)$  in the  $0.25 \text{ mol} \cdot \text{L}^{-1}$  GALd+ $0.25 \text{ mol} \cdot \text{L}^{-1}$  MA+ $0.25 \text{ mol} \cdot \text{L}^{-1}$  Gly reaction, which were both alkaline conditions (Fig. 4). The color of the GALd+Gly solution changed from colorless to bright yellow and finally to dark brown. A drastic BrC formation could be observed (Fig. 5), which was similar to that of the GALd+MA+Gly reaction.

Tab. 1 The first-order reaction rate constants ( $k$ ) of GALd and MA, Gly, the mixture of two types of species among AS, MA, and Gly at 216 nm and 330 nm

Reactions	216 nm		330 nm	
	$k/s^{-1}$	$R^2$	$k/s^{-1}$	$R^2$
GALd+MA	$2.73 \times 10^{-6}$	0.89	$3.08 \times 10^{-6}$	0.92
GALd+MA+AS	$1.94 \times 10^{-6}$	0.88	$1.88 \times 10^{-6}$	0.92
GALd+Gly	$3.14 \times 10^{-6}$	0.97	$3.45 \times 10^{-6}$	0.97
GALd+Gly+AS	$2.39 \times 10^{-6}$	0.91	$2.65 \times 10^{-6}$	0.93
GALd+MA+Gly	$1.90 \times 10^{-4}$	0.86	$1.24 \times 10^{-4}$	0.90

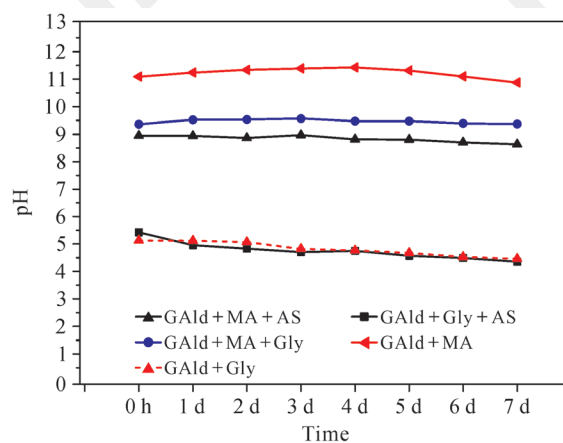


Fig. 3 The pH variations of GALd+MA+AS, GALd+Gly+AS, GALd+MA+Gly, GALd+MA, and GALd+Gly over time

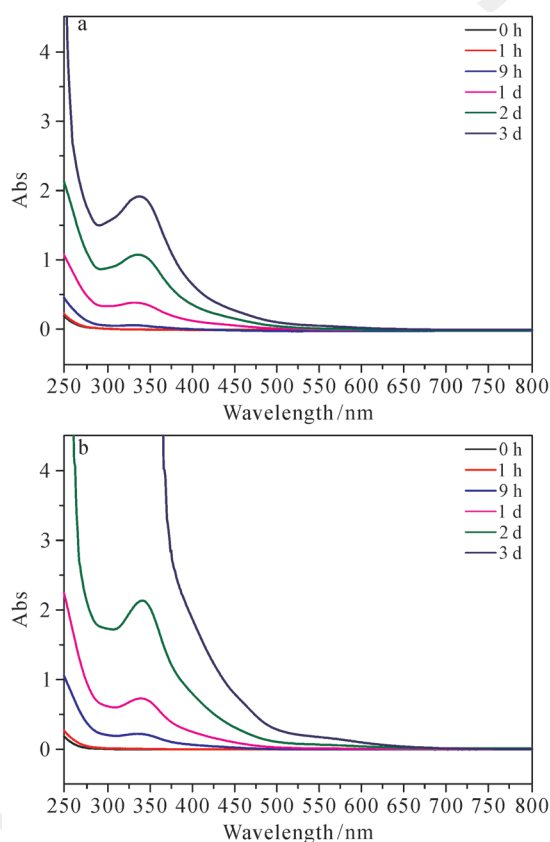


Fig. 4 The changes of UV-vis absorption from the reaction productions of  $0.2 \text{ mol} \cdot \text{L}^{-1}$  GALd+ $0.25 \text{ mol} \cdot \text{L}^{-1}$  Gly (a) and  $0.2 \text{ mol} \cdot \text{L}^{-1}$  GALd+ $0.25 \text{ mol} \cdot \text{L}^{-1}$  MA+ $0.25 \text{ mol} \cdot \text{L}^{-1}$  Gly (b)

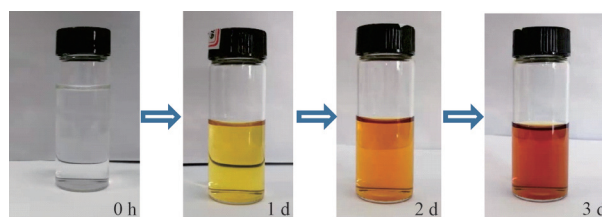


Fig. 5 The variations of solution color in the reaction of  $0.2 \text{ mol} \cdot \text{L}^{-1}$  GALd+ $0.25 \text{ mol} \cdot \text{L}^{-1}$  Gly at pH=9.43

### 2.3 The reaction mechanisms

Fig. 6 shows the LCMS-IT-TOF spectra of the reaction products of GALd+MA+AS, GALd+Gly+AS, and GALd+MA+Gly. In the GALd+MA+AS reaction, carbonium ion on the aldehyde group was nucleophilically attacked by the nitrogen atom on the amine group to form a Schiff base (Fig. 7a) (de Haan et al, 2009), which then underwent oligomerization reactions to form another product ( $m/z$  170). Moreover, the primary product  $m/z$  202  $[M+H]^+$  was produced by the product ( $m/z$  170) combined with one molecule of MA. Furthermore, two molecules of GALd could undergo the hemiacetal reaction, then couple with one molecule of  $NH_3$ , and lose two molecules of  $H_2O$  to form an imine with  $m/z$  101. The primary product with  $m/z$  272  $[M+H]^+$  was produced by the product ( $m/z$  170) reacting with imine ( $m/z$  101). The primary product with  $m/z$  217  $[M+K]^+$  was produced by the acetal of three molecules of GALd coupled with two molecules of  $NH_3$ , and then one molecule of  $H_2O$  was lost. Indeed,  $NH_3$  was a significant reactant in the GALd+MA+AS reaction. However, the GALd+ $NH_3$  products had no absorption at 330 nm (Fig. 2a), which would cause the reduction in the peak at 330 nm for GALd+MA because of the consumption of GALd as the reactant in the GALd+ $NH_3$  reaction. Moreover, AS could decrease the pH of the solution from  $(10.81 \pm 0.16)$  to  $(8.60 \pm 0.13)$  after it was added in GALd+MA (Fig. 3), which shifted Reaction (2) to the right and MA concentration decreased. It is easier for nitrogen in MA than that in  $CH_3NH_3^+$  to attack the carbonium because of higher electronegativity. The reduction in MA concentration might decline the reaction rate of GALd+MA and the reduction for the absorption peak at  $>300$  nm. Fig. 7b shows the reaction mechanisms of GALd+Gly+AS. The product detected at  $m/z$  201  $[M+H]^+$  was attributed to the product ( $m/z$  219) reacting with  $NH_3$  and then losing two molecules of  $H_2O$ . Here, the reaction mechanisms demonstrated that AS in the mixture could react with the GALd+Gly reaction products.

For the GALd+MA+Gly reaction, the primary product with  $m/z$  202  $[M+H]^+$  was produced by the

acetal of three molecules of GALd coupled with one molecule of Gly and then two molecules of  $H_2O$  were lost (Fig. 7c). Moreover, three molecules of GALd coupled with MA and lost one or two molecules of  $H_2O$  to form the products with  $m/z$  175 and  $m/z$  157. Furthermore, one molecule of Gly reacted with one molecule of MA to form the product with  $m/z$  88, which coupled with the products with  $m/z$  175 and  $m/z$  157, and then one molecule of  $H_2O$  was lost, respectively, to form the products with  $m/z$  246  $[M+H]^+$  and 228  $[M+H]^+$ . The product with  $m/z$  259  $[M+H]^+$  was produced by the product with  $m/z$  227 coupled with one molecule of MA. The product detected at  $m/z$  303  $[M+H]^+$  was attributed to the product ( $m/z$  227) reacting with Gly ( $m/z$  75). The product with  $m/z$  259  $[M+H]^+$  was produced through another pathway in which four molecules of GALd underwent acetal reaction and then coupled with two molecules of  $H_2O$ . Obviously, Gly participated in the reaction. When Gly was added to the GALd+MA solution, for the GALd+Gly reaction system, Reaction (3) shifted to the right because of higher pH (Fig. 3) and the  $H_2NCH_2COO^-$  concentration increased. There is a greater electronegativity for nitrogen in  $H_2NCH_2COO^-$  than that in  $H_2NCH_2COOH$ . Therefore, it is easier to attack carbonium ion for  $H_2NCH_2COO^-$  than Gly. With the addition of  $H_2NCH_2COO^-$ , the GALd+ $H_2NCH_2COO^-$  reaction might contribute high absorption at  $>300$  nm even a huge absorption because of the sharp pH increase.

### 2.4 Formed aqueous SOC evaluation

Thermal fractions of OC differ by sources (Watson et al, 1994; Chow et al, 2004; Niu et al, 2013) and have been used for the source apportionment of carbonaceous aerosols (Kim et al, 2003; Cao et al, 2005). OC is divided into Pyrol C, Pk1 C, Pk2 C, Pk3 C, and Pk4 C in the thermal-optical carbon analyzer with an increase in temperature. The high-molecular-weight compounds with are harder to decompose; therefore, Pk4 C usually represents compounds with the highest molecular weights (MW) in five fractions. In this study, Pyrol C was derived from small molecules in the reactions of

GAlD with either AS, MA, or Gly and GAlD with MA+AS, Gly+AS, or MA+Gly. Tab. 2 shows the OC mass distributions of the GAlD+AS, GAlD+MA, GAlD+Gly, GAlD+MA+AS, GAlD+Gly+AS, and GAlD+MA+Gly reaction products in 7 d. From the table, GAlD, MA, and Gly were primarily distributed

in Pk1 C. Therefore, in these reactions, the OC masses in Pk2 C, Pk3 C, Pk4 C, and Pyrol C might be considered to be from the secondary formation. They were the lowest amount of SOC formed in the reactions when an assumption was made that Pk1 C in the reactions comes from the reactants.

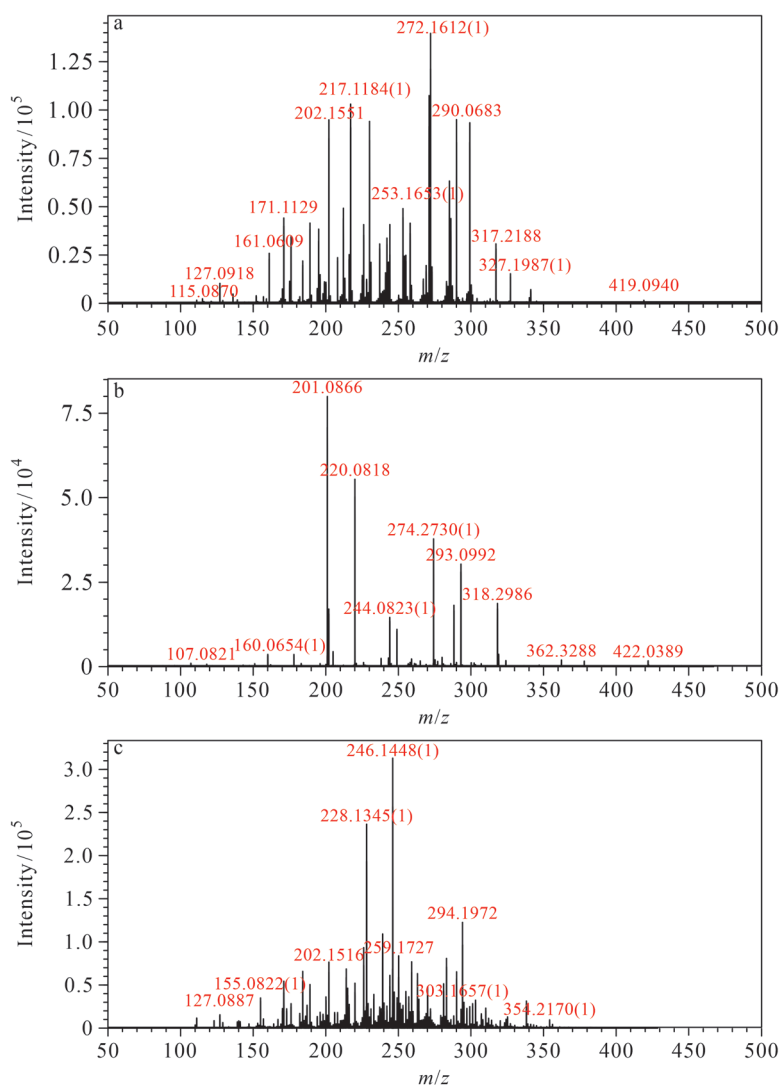


Fig. 6 LCMS-IT-TOF spectra of solutions containing GAlD+MA+AS (a), GAlD+Gly+AS (b), and GAlD+MA+Gly (c) under positive mode

Based on Tab. 2, compared with the SOC mass of GAlD+MA ( $1.24 \text{ g} \cdot \text{L}^{-1}$  in 7 d), after AS was added into the GAlD+MA reaction, there was a higher SOC mass ( $3.69 \text{ g} \cdot \text{L}^{-1}$  in 7 d). MA is a species with high volatility in the aqueous phase. MA in the GAlD+MA+AS mixed solution was considerably less volatile than that in GAlD+MA because of additional  $\text{CH}_3\text{NH}_3^+$  in

the aqueous phase with decrease in pH after AS was added. This might cause the SOC mass of GAlD+MA+AS to be higher than that of GAlD+MA. The relative contribution of each fraction SOC in the GAlD+MA+AS reaction followed an order of Pyrol C ( $58.3\%$ ) > Pk4 C ( $27.6\%$ ) > Pk2 C ( $7.6\%$ ) > Pk3 C ( $6.8\%$ ) in 7 d, indicating that most reaction products

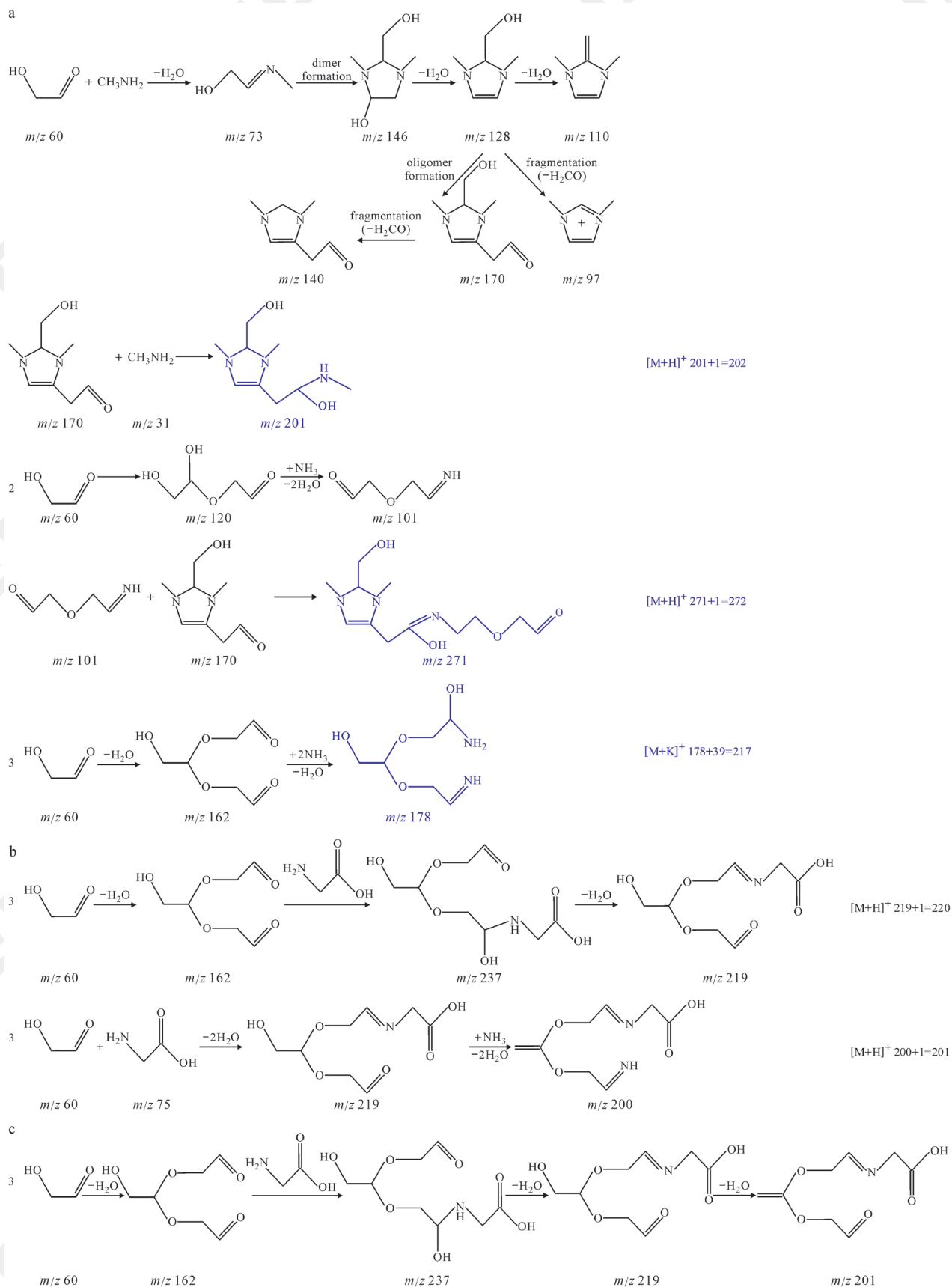
had small molecule weight. In the GALd+Gly+AS reaction, there was an increased SOC mass ( $6.60 \text{ g} \cdot \text{L}^{-1}$  in 7 d), contrary to that from the GALd+Gly reaction ( $4.52 \text{ g} \cdot \text{L}^{-1}$  in 7 d). The SOC mass distribution of the products from the GALd+Gly+AS reaction followed an order of Pyrol C (52.1%)>Pk4 C (27.4%)>Pk2 C (11.8%)>Pk3 C (8.8%) in 7 d, indicating that the low-molecular-weight reaction products were dominant. The GALd+MA+Gly mixture ( $5.77 \text{ g} \cdot \text{L}^{-1}$  in 7 d) demonstrated higher SOC mass than those from the reactions of GALd+MA ( $1.24 \text{ g} \cdot \text{L}^{-1}$  in 7 d) and GALd+Gly ( $4.52 \text{ g} \cdot \text{L}^{-1}$  in 7 d). In the GALd+MA+Gly reaction, compared with the SOC mass of GALd+MA or GALd+Gly reaction products, there was a significant increase in SOC formation. The SOC mass distribution followed an order of Pk2 C (36.6%)>Pyrol C (32.9%)>Pk4 C (20.1%)>Pk3 C (10.4%) in 7 d. From the abovementioned results, after AS was added into GALd+MA or GALd+Gly and after Gly was added into GALd+MA, there was higher SOC mass in the aqueous phase than those from GALd+MA or GALd+Gly.

Note that, from Tab. 2, the ratio of SOC with the relatively high MW (Pk3 C+Pk4 C) of the GALd+MA+AS reaction was 34.4%, higher than that of the GALd+MA reaction (31.8%). Similarly, the high MW SOC (Pk3 C+Pk4 C) occupied 36.1% in the produced SOC from the GALd+Gly+AS reaction, which was greater than that from the GALd+Gly reaction (32.3%). In these two reactions, AS participated in the reactions as reactants. Different from them, in the GALd+MA+Gly reaction, higher SOC mass was produced than in the GALd+MA and GALd+Gly reactions; however, the percentage of SOC mass with high MW was relatively low. Interestingly, in this study, the highest percentage of SOC mass occurred with high MW in produced SOC from the GALd+AS reaction among all reactions. Therefore, it could be speculated that in the reaction of GALd with ammonium/amine, after AS participated in the reaction, high MW products tended to form.

## 2.5 Atmospheric implications

GALd is a sufficiently water-soluble carbonyl

compound with an effective Henry's constant ( $H^* = 0.41 \times e^{[4.6 \times 10^3(1/7 - 1/298)]} \text{ mol} \cdot \text{L}^{-1} \cdot \text{Pa}^{-1}$ ). AS is an important component of global anthropogenic aerosols with a concentration of  $3200\text{--}7700 \text{ pmol} \cdot \text{m}^{-3}$  in the aerosols (Matsumoto and Uematsu, 2005). MA, the smallest alkyl amine in the atmosphere, has the highest emission in the globe, which has been detected in aerosols with a concentration of  $(56 \pm 52) \text{ pmol} \cdot \text{m}^{-3}$ . Gly is a representative dissolved free amino acid with the simplest structure of all dissolved free amino acids. The Gly concentration ranges from  $0.2$  to  $170 \text{ pmol} \cdot \text{m}^{-3}$  in aerosols (Zhang and Anastasio, 2003; Matsumoto and Uematsu, 2005). GALd in aerosol particles could react with two types of species among AS, MA, and Gly and produced BrC. Fig. 8 shows the MAC of reactions of GALd and single MA and Gly and GALd with MA+AS, Gly+AS, and MA+Gly. From the figure, the MAC at 330 nm ( $\text{MAC}_{330}$ ) with the GALd+MA+AS and GALd+Gly+AS reactions were  $38.4 \text{ cm}^2 \cdot \text{g}^{-1}$  and  $147 \text{ cm}^2 \cdot \text{g}^{-1}$  after 7 d, respectively, whereas that of GALd+MA+Gly after 7 d was  $5.98 \times 10^3 \text{ cm}^2 \cdot \text{g}^{-1}$ . In comparison, the  $\text{MAC}_{330}$  of products from the GALd+MA and GALd+Gly reactions were  $716 \text{ cm}^2 \cdot \text{g}^{-1}$  and  $356 \text{ cm}^2 \cdot \text{g}^{-1}$ , respectively. Obviously, the MAC of products reduced when AS was added in the GALd+MA or GALd+Gly reaction, whereas, when Gly was added into the GALd+MA reaction, the MAC of products increased, suggesting the inhibitory effect of AS and the synergistic effect of Gly in the reactions of GALd with amines to form BrC. Therefore, where there were high concentrations of carbonyl compounds and amines, e.g., in the urban and forest areas (Ortiz et al, 2006; Volkamer et al, 2007), and in rural and marine areas (O'Neill and Phillips, 1992; Schade and Crutzen, 1995; Calderón et al, 2007; Dai et al, 2012), there would be additional BrC in the atmospheric particles, which will result in additional radiative forcing. While where there was a high concentration AS, such as in the urban areas in North China Plain (Cao et al, 2017), BrC formation from GALd with amines would be inhibited. These results significant implications on BrC formation in the atmosphere, the contribution of GALd to BrC formation in chemical models, and the predictions of the behaviors of other carbonyls in the atmosphere.



(To be continued)

(Continued Fig. 7c)

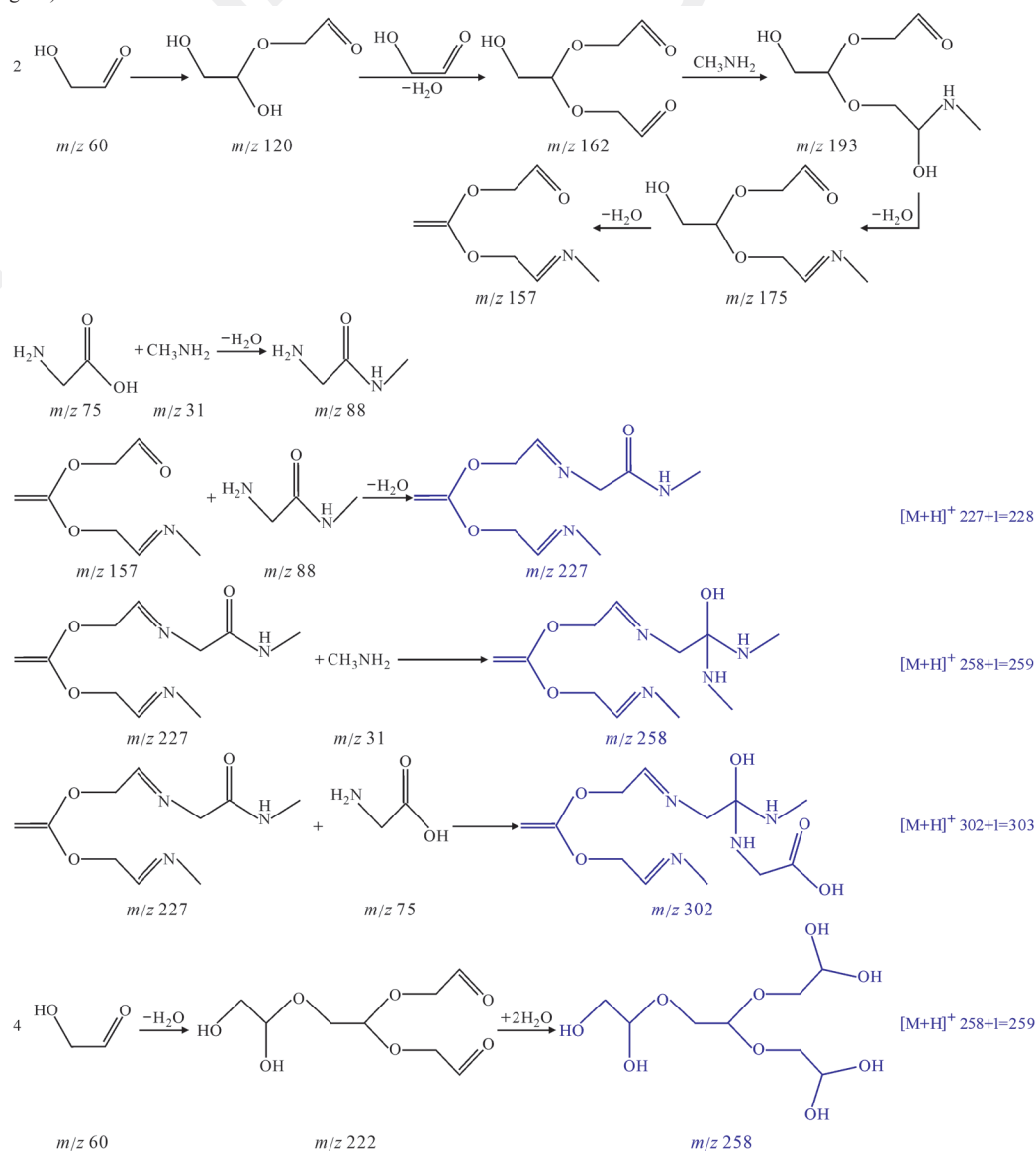


Fig. 7 Possible reactions occurring in the GAld+MA+AS (a), GAld+Gly+AS (b) and GAld+MA+Gly (c) in 7 d (blue colored compounds were identified in this study)

Tab. 2 The OC mass and distribution of separate  $0.2 \text{ mol}\cdot\text{L}^{-1}$  GAld,  $0.25 \text{ mol}\cdot\text{L}^{-1}$  AS,  $0.25 \text{ mol}\cdot\text{L}^{-1}$  MA, and  $0.25 \text{ mol}\cdot\text{L}^{-1}$  Gly and the reactions of  $0.2 \text{ mol}\cdot\text{L}^{-1}$  GAld+ $0.25 \text{ mol}\cdot\text{L}^{-1}$  AS,  $0.2 \text{ mol}\cdot\text{L}^{-1}$  GAld+ $0.25 \text{ mol}\cdot\text{L}^{-1}$  MA,  $0.2 \text{ mol}\cdot\text{L}^{-1}$  GAld+ $0.25 \text{ mol}\cdot\text{L}^{-1}$  Gly,  $0.2 \text{ mol}\cdot\text{L}^{-1}$  GAld+ $0.25 \text{ mol}\cdot\text{L}^{-1}$  MA+ $0.25 \text{ mol}\cdot\text{L}^{-1}$  AS,  $0.2 \text{ mol}\cdot\text{L}^{-1}$  GAld+ $0.25 \text{ mol}\cdot\text{L}^{-1}$  Gly+ $0.25 \text{ mol}\cdot\text{L}^{-1}$  AS, and  $0.2 \text{ mol}\cdot\text{L}^{-1}$  GAld+ $0.25 \text{ mol}\cdot\text{L}^{-1}$  MA+ $0.25 \text{ mol}\cdot\text{L}^{-1}$  Gly in 7 d

Sample	OC $/(\text{g}\cdot\text{L}^{-1})$	SOC $/(\text{g}\cdot\text{L}^{-1})$	Pk1 C $/(\text{g}\cdot\text{L}^{-1})$	Pk2 C $/(\text{g}\cdot\text{L}^{-1})$	Pk3 C $/(\text{g}\cdot\text{L}^{-1})$	Pk4 C $/(\text{g}\cdot\text{L}^{-1})$	Pyrol C $/(\text{g}\cdot\text{L}^{-1})$	SOC with higher MW ratio in SOC Pk3 C+Pk4 C/%
GAld	3.95	0.05	3.90	0.05	0.01	0.00	-0.01	—
AS	0.01	0.00	0.01	0.01	0.00	0.00	-0.01	—
MA	-0.16	-0.36	0.20	-0.08	-0.06	-0.12	-0.10	—
Gly	4.92	0.37	4.55	0.20	0.11	0.05	0.01	—
GAld+AS	4.07	0.72	3.35	0.15	0.07	0.40	0.09	65.6
GAld+MA	5.40	1.24	4.16	0.73	0.12	0.28	0.12	31.8
GAld+Gly	9.54	4.52	5.02	1.29	0.56	0.90	1.77	32.3
GAld+MA+AS	7.47	3.69	3.78	0.28	0.25	1.02	2.15	34.4
GAld+Gly+AS	9.65	6.60	3.05	0.78	0.58	1.81	3.44	36.1
GAld+MA+Gly	11.87	5.77	6.10	2.11	0.60	1.16	1.90	30.6

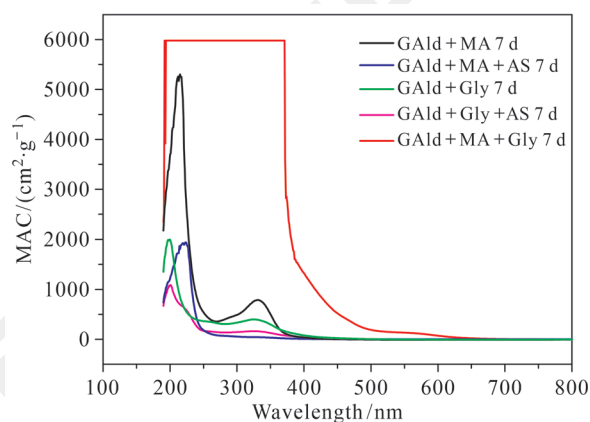


Fig. 8 The MAC of the GAld+MA, GAld+MA+AS, GAld+Gly, GAld+Gly+AS, and GAld+MA+Gly reaction products in 7 d

### 3 Conclusions

The influences of AS and Gly on reactions of GAld with amine were examined in the aqueous phase. The absorbance followed the orders of GAld+MA+AS < GAld+MA, GAld+Gly+AS < GAld+Gly, GAld+MA+Gly > GAld+MA or GAld+Gly. The reaction rate constants demonstrated the same patterns as those of the absorbance, suggesting AS played an inhibitory role, and the mixture of MA and Gly together had a synergistic effect on BrC formation. The primary reaction mechanisms were hemiacetal/acetal, nucleophilic attack, and additional complex high MW substance production from the polymerization of the formed Schiff imine. Moreover, AS participated in the GAld+MA and GAld+Gly reactions. After AS or Gly was added, additional SOC mass in the mixed reaction was produced than those of GAld with single MA and Gly. AS favored the production of high MW SOC in the reactions of GAld with amines.

### References

Bacher C, Tyndall G S, Orlando J J. 2001. The atmospheric chemistry of glycolaldehyde [J]. *Journal of Atmospheric Chemistry*, 39(2): 171–189.

Birch M E, Cary R A. 1996. Elemental carbon-based method for monitoring occupational exposures to particulate diesel exhaust [J]. *Aerosol Science and Technology*, 25(3): 221–241.

Bond T C. 2001. Spectral dependence of visible light absorption by carbonaceous particles emitted from coal combustion [J]. *Geophysical Research Letters*, 28(21): 4075–4078.

Bones D L, Henricksen D K, Mang S A, et al. 2010. Appearance of strong absorbers and fluorophores in limonene-O<sub>3</sub> secondary organic aerosol due to NH<sub>4</sub><sup>+</sup>-mediated chemical aging over long time scales [J]. *Journal of Geophysical Research: Atmospheres*, 115(D5): D05203. DOI: 10.1029/2009JD012864.

Calderón S M, Poor N D, Campbell S W. 2007. Estimation of the particle and gas scavenging contributions to wet deposition of organic nitrogen [J]. *Atmospheric Environment*, 41(20): 4281–4290.

Cao J J, Wu F, Chow J C, et al. 2005. Characterization and source apportionment of atmospheric organic and elemental carbon during fall and winter of 2003 in Xi'an, China [J]. *Atmospheric Chemistry and Physics*, 5(11): 3127–3137.

Cao Z Y, Zhou X H, Ma Y J, et al. 2017. The concentrations, formations, relationships and modeling of sulfate, nitrate and ammonium (SNA) aerosols over China [J]. *Aerosol and Air Quality Research*, 17(1): 84–97.

Chen Q C, Hua X Y, Dyussenova A. 2021a. Evolution of the chromophore aerosols and its driving factors in summertime Xi'an, northwest China [J]. *Chemosphere*, 281: 130838. DOI: 10.1016/j.chemosphere.2021.130838.

Chen Q C, Hua X Y, Li J W, et al. 2021b. Diurnal evolutions and sources of water-soluble chromophoric aerosols over Xi'an during haze event, in northwest China [J]. *Science of the Total Environment*, 786: 147412. DOI: 10.1016/j.scitotenv.2021.147412.

Chow J C, Watson J G, Chen L W A, et al. 2004. Equivalence of elemental carbon by thermal/optical reflectance and transmittance with different temperature protocols [J]. *Environmental Science & Technology*, 38(16): 4414–4422.

Dai W T, Ho S S H, Ho K F, et al. 2012. Seasonal and diurnal variations of mono- and di-carbonyls in Xi'an, China [J]. *Atmospheric Research*, 113: 102–112.

de Haan D O, Corrigan A L, Smith K W, et al. 2009. Secondary organic aerosol-forming reactions of glyoxal with amino acids [J]. *Environmental Science & Technology*, 43(8): 2818–2824.

de Haan D O, Hawkins L N, Kononenko J A, et al. 2011.

- Formation of nitrogen-containing oligomers by methylglyoxal and amines in simulated evaporating cloud droplets [J]. *Environmental Science & Technology*, 45(3): 984–991.
- de Haan D O, Jansen K, Rynaski A D, et al. 2020. Brown carbon production by aqueous-phase interactions of glyoxal and SO<sub>2</sub> [J]. *Environmental Science & Technology*, 54(8): 4781–4789.
- de Haan D O, Tapavicza E, Riva M, et al. 2018. Nitrogen-containing, light-absorbing oligomers produced in aerosol particles exposed to methylglyoxal, photolysis, and cloud cycling [J]. *Environmental Science & Technology*, 52(7): 4061–4071.
- Fu T M, Jacob D J, Wittrock F, et al. 2008. Global budgets of atmospheric glyoxal and methylglyoxal, and implications for formation of secondary organic aerosols [J]. *Journal of Geophysical Research: Atmospheres*, 113(D15): D15303. DOI: 10.1029/2007JD009505.
- Galano A, Alvarez-Idaboy J R, Ruiz-Santoyo M E, et al. 2004. Mechanism and kinetics of the reaction of OH radicals with glyoxal and methylglyoxal: a quantum Chemistry+CVT/SCT approach [J]. *ChemPhysChem*, 5(9): 1379–1388.
- Galloway M M, Chhabra P S, Chan A W H, et al. 2009. Glyoxal uptake on ammonium sulphate seed aerosol: reaction products and reversibility of uptake under dark and irradiated conditions [J]. *Atmospheric Chemistry and Physics*, 9(10): 3331–3345.
- Goldstein A H, Galbally I E. 2007. Known and unknown organic constituents in the Earth's atmosphere [J]. *Environmental Science & Technology*, 41(5): 1514–1521.
- Hastings W P, Koehler C A, Bailey E L, et al. 2005. Secondary organic aerosol formation by glyoxal hydration and oligomer formation: humidity effects and equilibrium shifts during analysis [J]. *Environmental Science & Technology*, 39(22): 8728–8735.
- Hecobian A, Zhang X, Zheng M, et al. 2010. Water-soluble organic aerosol material and the light-absorption characteristics of aqueous extracts measured over the Southeastern United States [J]. *Atmospheric Chemistry and Physics*, 10(13): 5965–5977.
- Jimenez N G, Sharp K D, Gramyk T, et al. 2022. Radical-initiated brown carbon formation in sunlit carbonyl-amine-ammonium sulfate mixtures and aqueous aerosol particles [J]. *ACS Earth and Space Chemistry*, 6(1): 228–238.
- Kawamura K, Okuzawa K, Aggarwal S G, et al. 2013. Determination of gaseous and particulate carbonyls (glycolaldehyde, hydroxyacetone, glyoxal, methylglyoxal, nonanal and decanal) in the atmosphere at Mt. Tai [J]. *Atmospheric Chemistry and Physics*, 13(10): 5369–5380.
- Kim E, Larson T V, Hopke P K, et al. 2003. Source identification of PM<sub>2.5</sub> in an arid northwest U.S. city by positive matrix factorization [J]. *Atmospheric Research*, 66(4): 291–305.
- Kirchstetter T W, Novakov T, Hobbs P V. 2004. Evidence that the spectral dependence of light absorption by aerosols is affected by organic carbon [J]. *Journal of Geophysical Research: Atmospheres*, 109(D21): D21208. DOI: 10.1029/2004JD004999.
- Kua J, Galloway M M, Millage K D, et al. 2013. Glycolaldehyde monomer and oligomer equilibria in aqueous solution: comparing computational chemistry and NMR data [J]. *The Journal of Physical Chemistry A*, 117(14): 2997–3008.
- Lack D A, Langridge J M, Bahreini R, et al. 2012. Brown carbon and internal mixing in biomass burning particles [J]. *Proceedings of the National Academy of Sciences of the United States of America*, 109(37): 14802–14807.
- Laskin A, Laskin J, Nizkorodov S A. 2015. Chemistry of atmospheric brown carbon [J]. *Chemical Reviews*, 115(10): 4335–4382.
- Matsumoto K, Uematsu M. 2005. Free amino acids in marine aerosols over the western North Pacific Ocean [J]. *Atmospheric Environment*, 39(11): 2163–2170.
- Niu Z C, Wang S, Chen J S, et al. 2013. Source contributions to carbonaceous species in PM<sub>2.5</sub> and their uncertainty analysis at typical urban, peri-urban and background sites in southeast China [J]. *Environmental Pollution*, 181: 107–114.
- Nozière B, Esteve W. 2007. Light-absorbing aldol condensation products in acidic aerosols: spectra, kinetics, and contribution to the absorption index [J]. *Atmospheric Environment*, 41(6): 1150–1163.
- O'Neill D H, Phillips V R. 1992. A review of the control of odour nuisance from livestock buildings: part 3, properties of the odorous substances which have been identified in livestock wastes or in the air around them [J]. *Journal of*

- Agricultural Engineering Research*, 53: 23–50.
- Ortiz R, Hagino H, Sekiguchi K, et al. 2006. Ambient air measurements of six bifunctional carbonyls in a suburban area [J]. *Atmospheric Research*, 82(3/4): 709–718.
- Perri M J, Seitzinger S, Turpin B J. 2009. Secondary organic aerosol production from aqueous photooxidation of glycolaldehyde: laboratory experiments [J]. *Atmospheric Environment*, 43(8): 1487–1497.
- Powelson M H, Espelien B M, Hawkins L N, et al. 2014. Brown carbon formation by aqueous-phase carbonyl compound reactions with amines and ammonium sulfate [J]. *Environmental Science & Technology*, 48(2): 985–993.
- Schade G W, Crutzen P J. 1995. Emission of aliphatic amines from animal husbandry and their reactions: potential source of N<sub>2</sub>O and HCN [J]. *Journal of Atmospheric Chemistry*, 22(3): 319–346.
- Schwier A N, Sareen N, Mitroo D, et al. 2010. Glyoxal-methylglyoxal cross-reactions in secondary organic aerosol formation [J]. *Environmental Science & Technology*, 44(16): 6174–6182.
- Shapiro E L, Szprengiel J, Sareen N, et al. 2009. Light-absorbing secondary organic material formed by glyoxal in aqueous aerosol mimics [J]. *Atmospheric Chemistry and Physics*, 9(7): 2289–2300.
- Sørensen P E. 1972. The reversible addition of water to glycolaldehyde in aqueous solution [J]. *Acta Chemica Scandinavica*, 26(8): 3357–3365.
- Spaulding R S, Schade G W, Goldstein A H, et al. 2003. Characterization of secondary atmospheric photooxidation products: evidence for biogenic and anthropogenic sources [J]. *Journal of Geophysical Research Atmospheres*, 108(D8): 4247. DOI: 10.1029/2002JD002478.
- Tang J, Wang J Q, Zhong G C, et al. 2021. Measurement report: long-emission-wavelength chromophores dominate the light absorption of brown carbon in aerosols over Bangkok: impact from biomass burning [J]. *Atmospheric Chemistry and Physics*, 21(14): 11337–11352.
- Volkamer R, San Martini F, Molina L T, et al. 2007. A missing sink for gas-phase glyoxal in Mexico City: formation of secondary organic aerosol [J]. *Geophysical Research Letters*, 34(19): L19807. DOI: 10.1029/2007GL030752.
- Warneck P. 2003. In-cloud chemistry opens pathway to the formation of oxalic acid in the marine atmosphere [J]. *Atmospheric Environment*, 37(17): 2423–2427.
- Watson J G, Chow J C, Lowenthal D H, et al. 1994. Differences in the carbon composition of source profiles for diesel- and gasoline-powered vehicles [J]. *Atmospheric Environment*, 28(15): 2493–2505.
- Yi Y Y, Cao Z Y, Zhou X H, et al. 2018a. Formation of aqueous-phase secondary organic aerosols from glycolaldehyde and ammonium sulfate/amines: a kinetic and mechanistic study [J]. *Atmospheric Environment*, 181: 117–125.
- Yi Y Y, Zhou X H, Xue L K, et al. 2018b. Air pollution: formation of brown, light-absorbing, secondary organic aerosols by reaction of hydroxyacetone and methylamine [J]. *Environmental Chemistry Letters*, 16(3): 1083–1088.
- Yu G, Bayer A R, Galloway M M, et al. 2011. Glyoxal in aqueous ammonium sulfate solutions: products, kinetics and hydration effects [J]. *Environmental Science & Technology*, 45(15): 6336–6342.
- Zhang Q, Anastasio C. 2003. Free and combined amino compounds in atmospheric fine particles (PM<sub>2.5</sub>) and fog waters from northern California [J]. *Atmospheric Environment*, 37(16): 2247–2258.
- Zhang X L, Lin Y H, Surratt J D, et al. 2011. Light-absorbing soluble organic aerosol in Los Angeles and Atlanta: a contrast in secondary organic aerosol [J]. *Geophysical Research Letters*, 38(21): L21810. DOI: 10.1029/2011GL049385.
- Zhou X L, Huang G, Civerolo K, et al. 2009. Measurement of atmospheric hydroxyacetone, glycolaldehyde, and formaldehyde [J]. *Environmental Science & Technology*, 43(8): 2753–2759.